CHINA FOUNDRY Research & Development
Vol. 23 No. 1 January 2026
www.springer.com/41230
https://doi.org/10.1007/s41230-026-5020-x

Automatic gating and riser system design and defect control for K4169 superalloy guide blade casting based on parametric 3D modeling-simulation integrated system

Le-chuan Li[1], *Ya-jun Yin[1], Bing-zheng Fan[2], Guo-yan Shui[2], Xiao-yuan Ji[1], Jian-xin Zhou[1], and Lei Jin[2]

1. State Key Laboratory of Materials Processing and Die & Mould Technology, Huazhong University of Science and Technology, Wuhan 430074, China

2. Shenyang Research Institute of Foundry Co., Ltd. CAM, Shenyang 110022, China

Abstract: Automation and intelligence have become the primary trends in the design of investment casting processes. However, the design of gating and riser systems still lacks precise quantitative evaluation criteria. Numerical simulation plays a significant role in quantitatively evaluating current processes and making targeted improvements, but its limitations lie in the inability to dynamically reflect the formation outcomes of castings under varying process conditions, making real-time adjustments to gating and riser designs challenging. In this study, an automated design model for gating and riser systems based on integrated parametric 3D modeling-simulation framework is proposed, which enhances the flexibility and usability of evaluating the casting process by simulation. Firstly, geometric feature extraction technology is employed to obtain the geometric information of the target casting. Based on this information, an automated design framework for gating and riser systems is established, incorporating multiple structural parameters for real-time process control. Subsequently, the simulation results for various structural parameters are analyzed, and the influence of these parameters on casting formation is thoroughly investigated. Finally, the optimal design scheme is generated and validated through experimental verification. Simulation analysis and experimental results show that using a larger gate neck (24 mm in side length) and external risers promotes a more uniform temperature distribution and a more stable flow state, effectively eliminating shrinkage cavities and enhancing process yield by 15%.

Keywords: numerical simulation; automatic design; investment casting; parametric 3D modeling; gating and riser system

CLC numbers: TG146.1+5 **Document code:** A **Article ID:** 1672-6421(2026)01-020-11

1 Introduction

Investment casting is one of the most important casting processes[1-2], widely utilized in manufacturing complex-structured components such as cases[3], aero-engines[4], turbine blades[5], and pumps[6]. The mold shell in investment casting offers a high degree of design freedom and exceptional processing accuracy, making it particularly suitable for producing castings with intricate curved surfaces and thin walls[7-9]. Guide blade castings, typical examples of complex structures, are employed in oxygen pump shells. Their primary function is to direct gas flow, which requires them to exhibit high surface accuracy, superior mechanical properties, and strong corrosion resistance[10-11]. With the large-scale production of superalloy investment castings, improving the qualification rate has become essential[12-15].

Numerical simulation is widely used in optimizing the investment casting process. Hu et al.[16] investigated the directional solidification and heat treatment processes of turbine blades using simulation. Wei et al.[17] employed simulation to study the lattice sandwich structure of nickel-based superalloys. Li et al.[18] predicted deformation in investment casting through

***Ya-jun Yin**

Male, born in 1985, Associate Professor, and doctoral supervisor. Research direction: Numerical simulation of casting.

E-mail: yinyajun436@hust.edu.cn

Received: 2025-01-22; Revised: 2025-05-30; Accepted: 2025-10-13

simulation. The above-mentioned work has demonstrated the effectiveness of numerical simulation in studying the forming mechanism of castings. Various physical processes of investment casting, including shell deformation[19], secondary dendrite arm spacing[20], core mechanical properties[21], thermal cracking[22], residual stress[23], and recrystallization[24], have been quantitatively analyzed using numerical simulation.

The design of gating and riser systems is critical to the success of investment casting processes. The gating system influences casting quality by regulating the position and flow rate during the filling process[25-27], while the riser system impacts defect formation, such as shrinkage cavities, by controlling the solidification and shrinkage behavior of castings[28-30].

In recent years, some new design techniques of gating and riser system have been proposed. Wang et al.[31] established a design model of response surface method to design the gating and riser system of open impellers. Compared with the conventional modulus method, the riser volume was reduced by 47.85% and the casting yield was increased by 15.02%. Wang et al.[25] proposed a new optimization method for gating system design using fruit fly optimization algorithm. Wang et al.[32] used numerical simulation technology to design the casting process of headstock castings. By extracting the average modulus and molten metal volume at the hot spot in the solidification simulation results, the feeder size was designed quantitatively. Vanikar et al.[33] developed a methodology for the design and optimization of an investment casting system based on genetic algorithms to enhance the accuracy and safety of the casting system through optimization of pouring parameters.

In previous research, the casting numerical simulation has two main functions, the first is to exclude some infeasible process schemes at the initial stage, and the second is to verify the designed process at the final stage. However, a key limitation of current simulation techniques in gating and riser design is their inability to dynamically reflect the effects of the casting process and facilitate real-time process adjustments. Numerical simulations are not involved in the quantitative optimization of the local structure of the gating and riser system due to the fact that the steps of 3D modeling and meshing cannot be seamlessly integrated with the process improvements[34], and such quantitative optimization is currently highly dependent on the personal experience of engineers. To address these challenges, it is essential to develop an adaptive, integrated system for parametric 3D modeling and simulation. This system can be embedded into numerical calculation modules to enhance the efficiency of large-scale simulation tasks. Additionally, such an integrated system forms a critical foundation for the integration of advanced technologies, including simulation-driven machine learning, digital twins[35], and other emerging innovations.

In this study, an automatic design model for gating and riser systems based on an integrated parametric 3D modeling-simulation framework of K4169 superalloy guide blades is proposed. Firstly, the 3D structure of the guide blade casting is analyzed using a structural feature extraction method. Next, the gating and riser processes are automatically designed within the integrated parametric modeling and simulation system. Subsequently, the processes are evaluated under varying structural parameters, with simulation results analyzed quantitatively. Finally, the optimal gating and riser processes are determined and validated through experimental verification.

2 Method and model

2.1 Casting analysis and geometric feature extraction

Figure 1 illustrates the structure of the casting studied in this study, a superalloy guide blade designed for the oxygen pump shell. The upper part of the casting features a hollow structure, which is thick and substantial. A rib plate connects the upper and lower layers, serving as the primary load-bearing component, which requires excellent mechanical performance. The middle section of the upper part contains blades, the critical functional area of the casting, demanding high precision. The lower part includes a thick and large region at its center, which is particularly prone to shrinkage. Consequently, this area requires special attention during the riser system design. Additionally, the sectional view of the blade reveals the casting's thinnest wall thickness (3 mm), which poses challenges for the smooth filling of molten metal.

The casting material used in this study is K4169 superalloy, a commonly utilized material for producing guide blade castings. K4169 alloy exhibits excellent fluidity and has a relatively narrow range of solidification temperature, which make it well-suited for investment casting processes. Table 1 lists the main chemical composition of K4169 alloy, while Table 2 provides its key physical parameters. The main defects of K4169 alloy in the casting process are shrinkage cavities and gas holes.

Firstly, the structural analysis and geometric feature extraction of the casting are performed. The 3D solid files are divided into finite difference meshes, which are then used to analyze the structural features. A key advantage of the mesh file is that each randomly generated point can be precisely located without the need to calculate the number of ray intersections to determine its exact position. Figure 2 illustrates the analysis process of structural features. In Fig. 2(a), a large number of random points are selected to calculate the central position of the model. Once the central position is determined, random points located on the casting's edge are used to calculate the distances from the longitudinal straight line passing through the central position. These distances represent the maximum radii of the casting at different layers, which are essential for designing the exterior dimensions of the riser system. Secondly, the smallest cube that fully encloses the casting is identified to determine its maximum size range in the x, y, and z dimensions, as shown in Fig. 2(b). Finally, a surface identification method is applied to calculate the area of the casting's outer surface. This calculation results are used to design the positions of the inner gates and risers, as shown in Fig. 2(c).

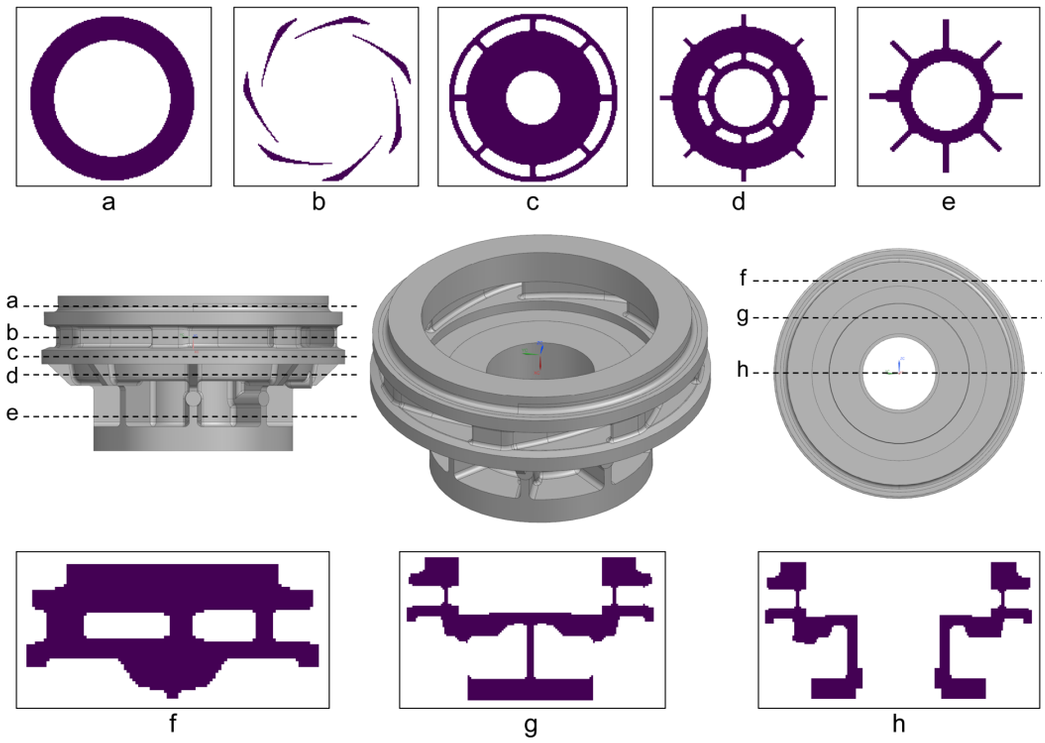

Fig. 1: Structural analysis of guide blade casting

Table 1: Elemental composition of K4169 alloy

Ni	Fe	C	Si	Mn	Cr	Al	Co	Cu	Nb	Ti
55.06	19	0.04	0.3	0.3	18	0.5	0.5	0.2	5.1	1

Table 2: Physical parameters of K4169 alloy

Density ($g \cdot cm^{-3}$)	Specific heat capacity $[Cal \cdot (g \cdot °C)^{-1}]$	Thermal conductivity $[Cal \cdot (cm \cdot s \cdot °C)^{-1}]$	Viscosity ($cm^2 \cdot s^{-1}$)	Latent heat ($Cal \cdot g^{-1}$)	Liquidus (°C)	Solidus (°C)	Shrinkage rate of phase transition
7.558	0.284	0.068	0.049	54.915	1366	1120	0.011

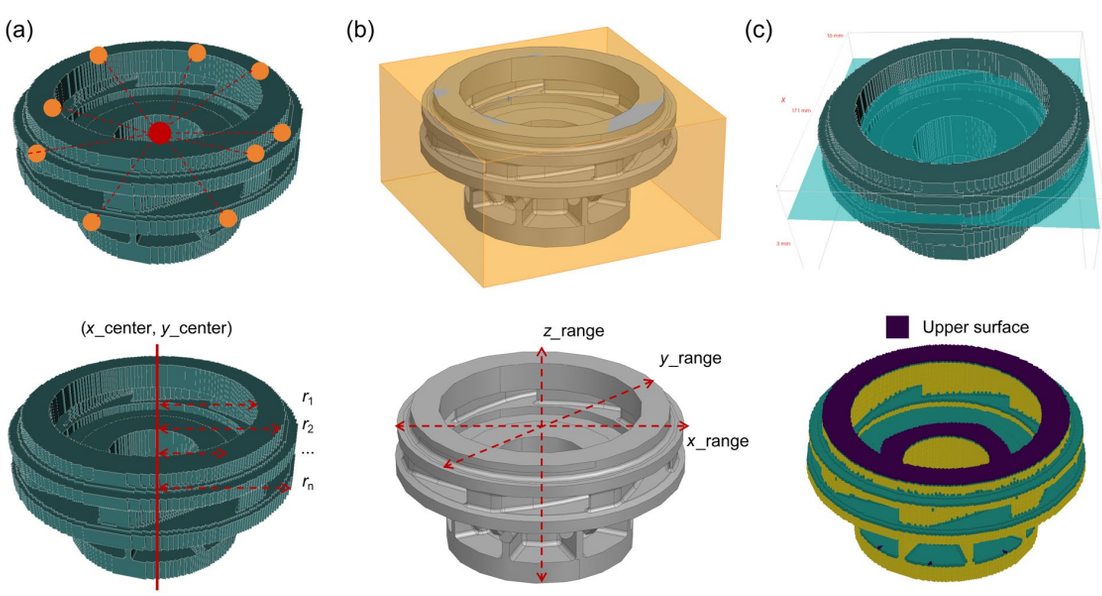

Fig. 2: Analysis of structural feature of the casting: (a) the calculation of center coordinates and the radius of each layer; (b) the calculation of the smallest cube that fully encloses the casting; (c) the calculation of the upper surface

2.2 Construction of automatic design framework for gating and riser system

An automated design framework for gating and riser systems, based on parametric 3D modeling, is constructed, as shown in Fig. 3. Figure 3(a) illustrates the geometric characterization of the casting obtained through structural feature extraction. Figure 3(b) presents the basic structural framework and parameters of the gating and riser systems, with the detailed specifications of the structural parameters provided in Table 3. Figure 3(c) depicts the automatic design process, which includes the following main steps: The geometric feature information of the casting is firstly analyzed to select appropriate components from the component library for assembly. Constraints are then established to ensure proper connections between individual components. These constraints ensure that the connections remain intact when size parameters change. Due to structural limitations, each structural parameter has upper and lower bounds, thus adjustments within these limits are needed to achieve optimal design results. The determination of these bounds also depends on the structural feature.

2.3 Establishment of integrated system of parametric 3D modeling and simulation

To achieve the integration of parametric 3D modeling and simulation, an integrated framework is established, as illustrated in Fig. 4. In this framework, the input consists of a set of structural parameters, each encompassing all the necessary parameters for the gating and riser system. Upon importing the structural parameters, grid files are batch-generated according to the rules defined for various structural configurations. The simulation model is constructed using InteCast CAE software. Table 4 presents the calculated parameters used in the simulation, along with the corresponding initial and boundary conditions. All simulation projects in this model share identical initial and boundary conditions, with the structure of the gating and riser system serving as the sole variable. This approach enables a focused study on the influence of different gating and riser designs on casting formation by controlling other calculated parameters. Following the simulation calculations, multiple sets of simulation results are generated. Each group of structural parameters corresponds to a unique simulation outcome, allowing for quantitative evaluation of the processes by comparing the simulation results across different structural configurations.

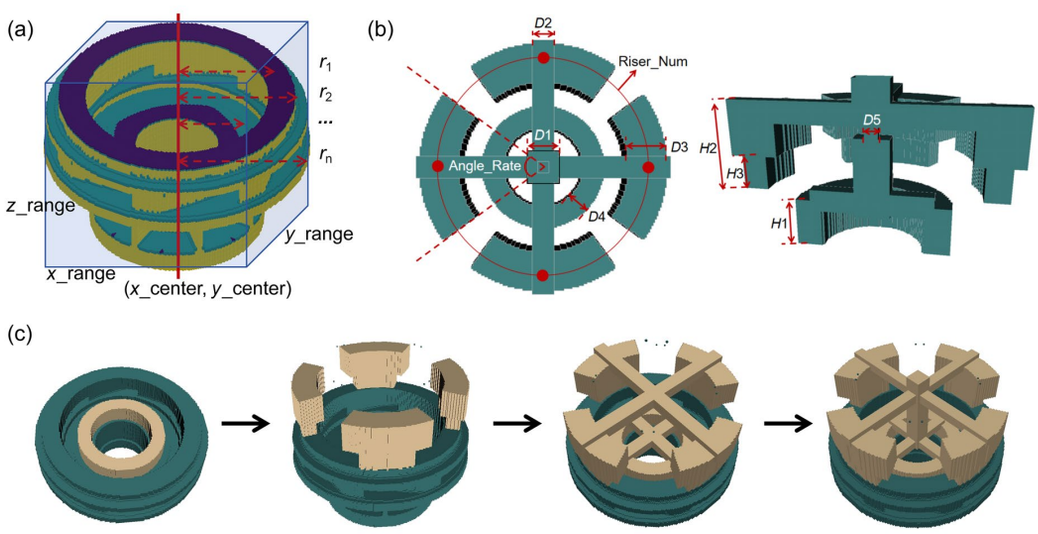

Fig. 3: Construction of automatic design framework for gating and riser system: (a) parameters obtained by structural analysis; (b) local dimensional parameters of gating and riser system; (c) generation steps of gating and riser system

Table 3: Illustration of structural parameters

Structural parameters	Illustration
*H*1 (mm)	Height of the internal risers
*H*2 (mm)	Total height of the external risers
*H*3 (mm)	Height of lower part of the external risers
*D*1 (mm)	Side length of the direct gate
*D*2 (mm)	Side length of the cross gates
*D*3 (mm)	Width of the external risers
*D*4 (mm)	Width of the internal risers
*D*5 (mm)	Side length of the contracted neck
Riser_Num	Amount of the external risers
Angle_Rate	Angle of riser/circle

3 Results and discussion

3.1 Automatic generation framework of gating and riser system

Figure 5 illustrates the results of the automatic generation framework for gating and riser systems, demonstrating that different configurations can be achieved by adjusting

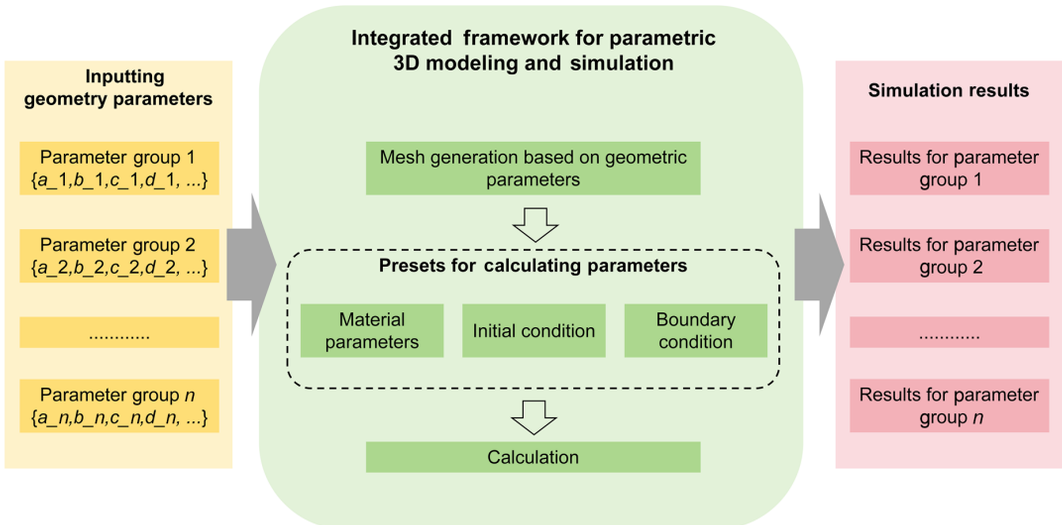

Fig. 4: Integrated framework for parametric 3D modeling and simulation

Table 4: Initial and boundary conditions for simulation

Temperature of casting (°C)	Temperature of shell mold (°C)	Thickness of shell mold (mm)	Interface heat transfer coefficient [W·(m²·K)$^{-1}$]	Thermal conductivity of shell mold [W·(m·K)$^{-1}$]
1,400	800	10	962.32	0.837

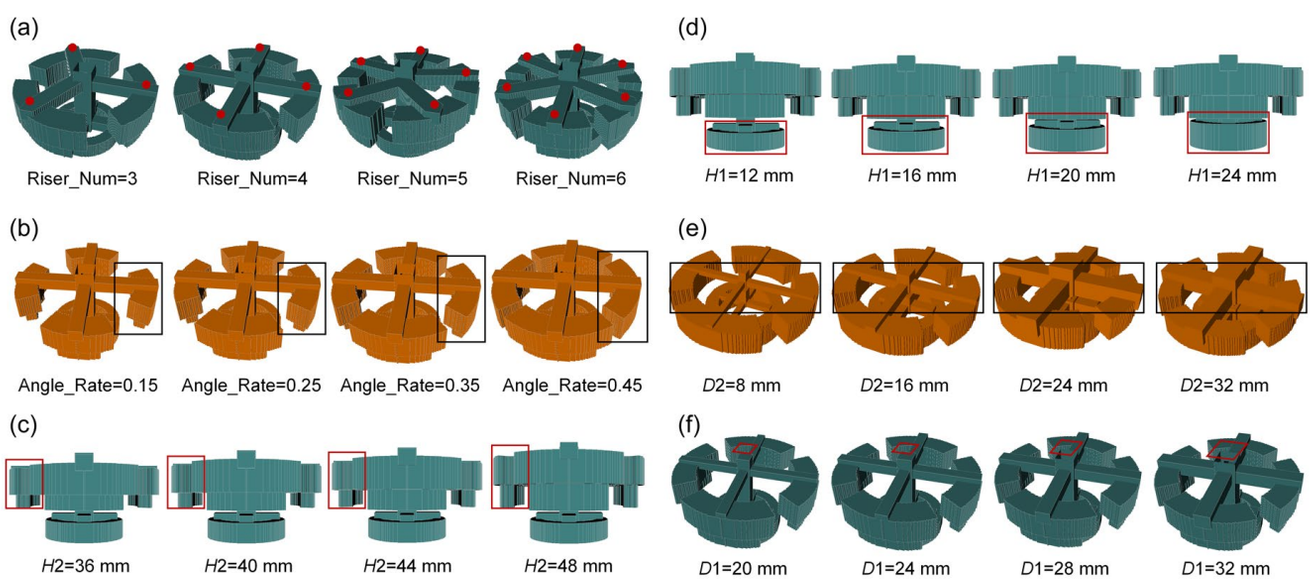

Fig. 5: Automatic design results of gating and riser systems with different parameters: (a) Riser_Num; (b) Angle_Rate; (c) *H*2; (d) *H*1; (e) *D*2; (f) *D*1

the structural parameters. Specifically, Figs. 5(a), (b), (c), and (d) show the automatic generation results for varying riser system parameters, while Figs. 5(e) and (f) display the results for different gating system parameters. The generated results confirm that the validity of the configurations remains intact when structural parameters are altered, thanks to the enforcement of structural constraints. Notably, the connection between the gating system and each riser is consistently maintained. As a result, thousands of gating and riser system configurations can be generated, provided the structural parameters are set within their permissible ranges. Among all the structural parameters, not all have a significant impact on casting formation. Therefore, several key structural parameters including gate neck sizes, cross gate sizes, external riser sizes, and internal riser sizes are selected to analyze the effects of different gating and riser processes on casting formation.

3.2 Influence of different structures of gating system on casting forming processes

In the design of the gating system, a specialized structure called the gate neck is used to divide the fluid flow. Figure 6 compares simulation results for different gate neck sizes, illustrating their obvious influence on the flow path. At the initial stage of flow, as shown in Fig. 6(a), when *D*5 is 24 mm,

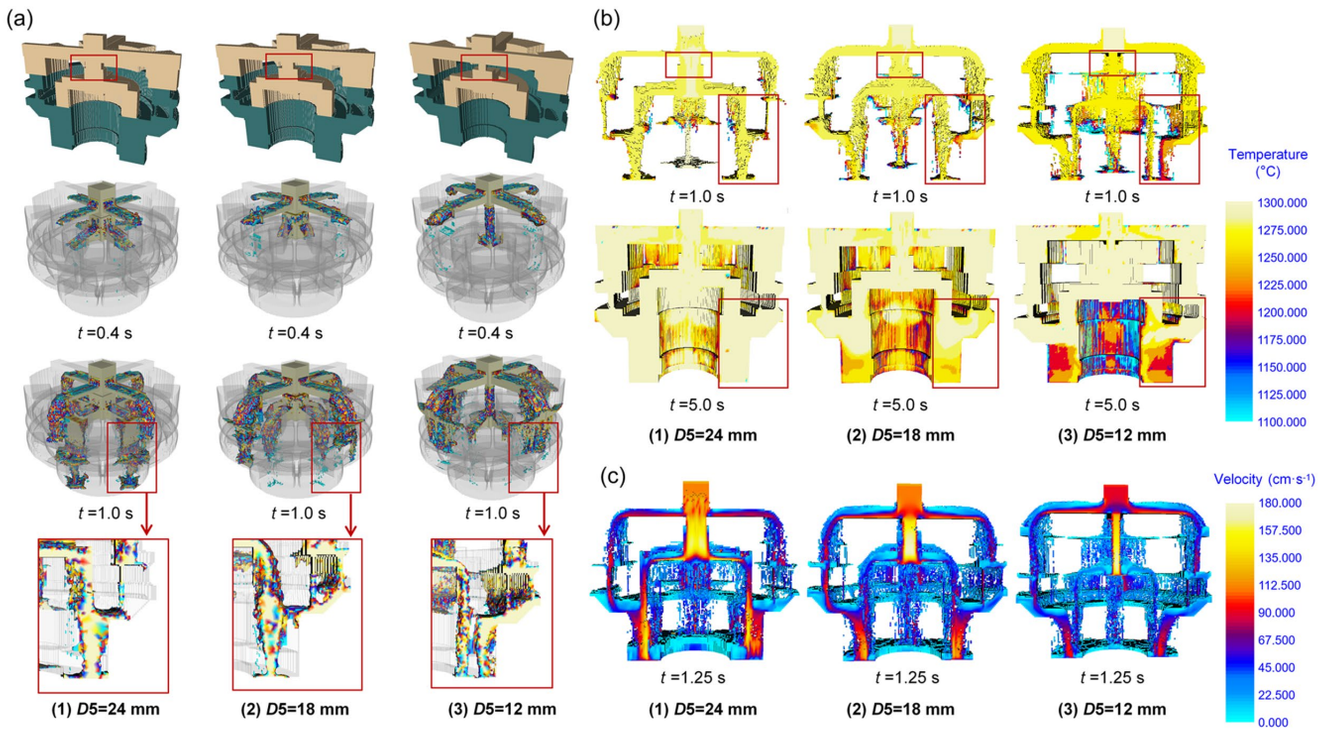

Fig. 6: Simulation results of flow process for different gate neck sizes in different values of *D*5: (a) filling process; (b) fluid temperature; (c) fluid velocity

a larger neck size directs most of the fluid into the lower internal riser, with comparatively less flowing into the upper external riser. The liquid metal entering the inner riser and that entering the outer riser meet at the bottom of the casting before eventually filling the shell. However, the size of the gate neck impacts the point where these two streams of liquid metal intersect. In the late filling stage depicted in the first condition (*D*5=24 mm) of Fig. 6(a), the inner liquid flow fills the bottom of the casting at first, while the outer flow is significantly slower. In contrast, in the third condition (*D*5=12 mm) of Fig. 6(a), the inner and outer flows nearly fill the bottom of the casting simultaneously. While this simultaneous filling ensures a relatively balanced overall temperature for the liquid metal, it increases the likelihood of gas entrapment at the intersection of the two streams. As a result, designs where the two streams meet simultaneously should be avoided to minimize this risk.

Gate neck of different sizes will also have an impact on the temperature distribution and frontier velocity of the casting flow. Figure 6(b) compares the temperature distribution of the internal section of the three processes at the same instant of the filling process. When *D*5 is relatively large, the temperature field distribution of the casting is relatively uniform, which is beneficial to reduce the residual stress and deformation. When *D*5 is small, the distribution of the temperature field is not uniform enough. However, for the solidification process of castings, the temperature field is more consistent with the temperature gradient of sequential solidification when *D*5 is small. It can enable the shrinkage cavity to be discharged more smoothly. Therefore, from the point of view of filling temperature field, the result is best when *D*5 is 18 mm. Figure 6(c) illustrates the difference in filling speeds of the three processes at the same time instant. It is clear that the larger the *D*5, the fast the overall filling speed, and all the high speed fluid comes from the middle channel. This leads to increased pressure on the middle part of the shell mold. At the same time, the higher filling speed will similarly lead to surface defects in the lower half of the casting, such as flow marks. On the contrary, in the case of the smallest *D*5 (12 mm), the fluid is all from the external channel, which also causes the non-uniform flow rate. In summary, the fluid velocity distribution is the most uniform for *D*5=18 mm.

Another key variable in the gating system design is the size of the cross gate. Figure 7 shows the comparison of simulation results for filling process with different cross gate sizes. From the flow regime of 0.6 s and 2.0 s, it can be seen that the filling speed is significantly accelerated by the increase of the size of the cross gate. The total filling time of the three processes is 9.91 s, 4.66 s, and 2.73 s, respectively. The faster filling speed can make the temperature of the liquid metal more uniform after filling the casting. At the same time, the faster filling speed will also lead to an increase in the pressure on the type shell, as shown in the Fig. 7(b). Compared with the case of *D*2=12 mm, the pressure at the bottom of the direct runner doubles at *D*2=28 mm, which results in a significant impact force on the shell and thereby challenges its mechanical properties. Figure 7(c) shows the shrinkage prediction results of the three schemes, and the shrinkage of the casting is significantly reduced with the increase of the size of the cross gate.

3.3 Influence of different structures of riser system on casting forming processes

Figure 8 presents a comparison of simulation results for mold

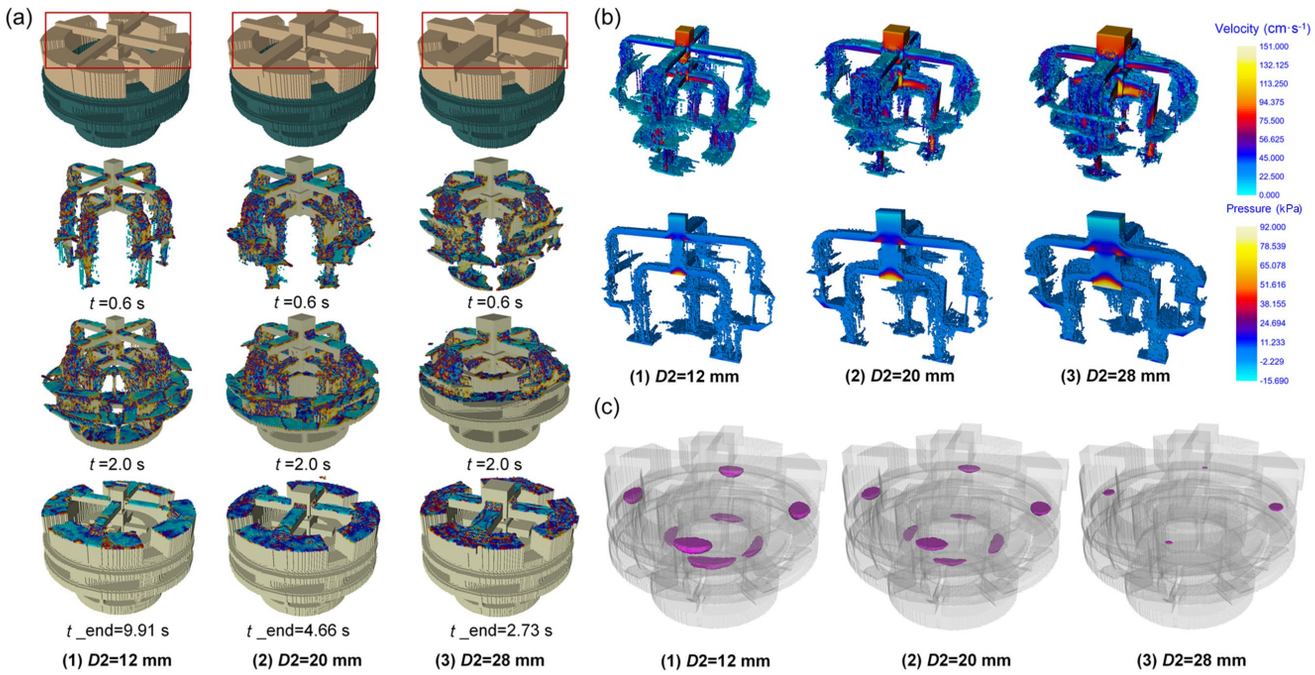

Fig. 7: Simulation results of flow process for different cross gate sizes in different values of *D*2: (a) filling process; (b) fluid velocity; (c) shrinkage cavity distribution

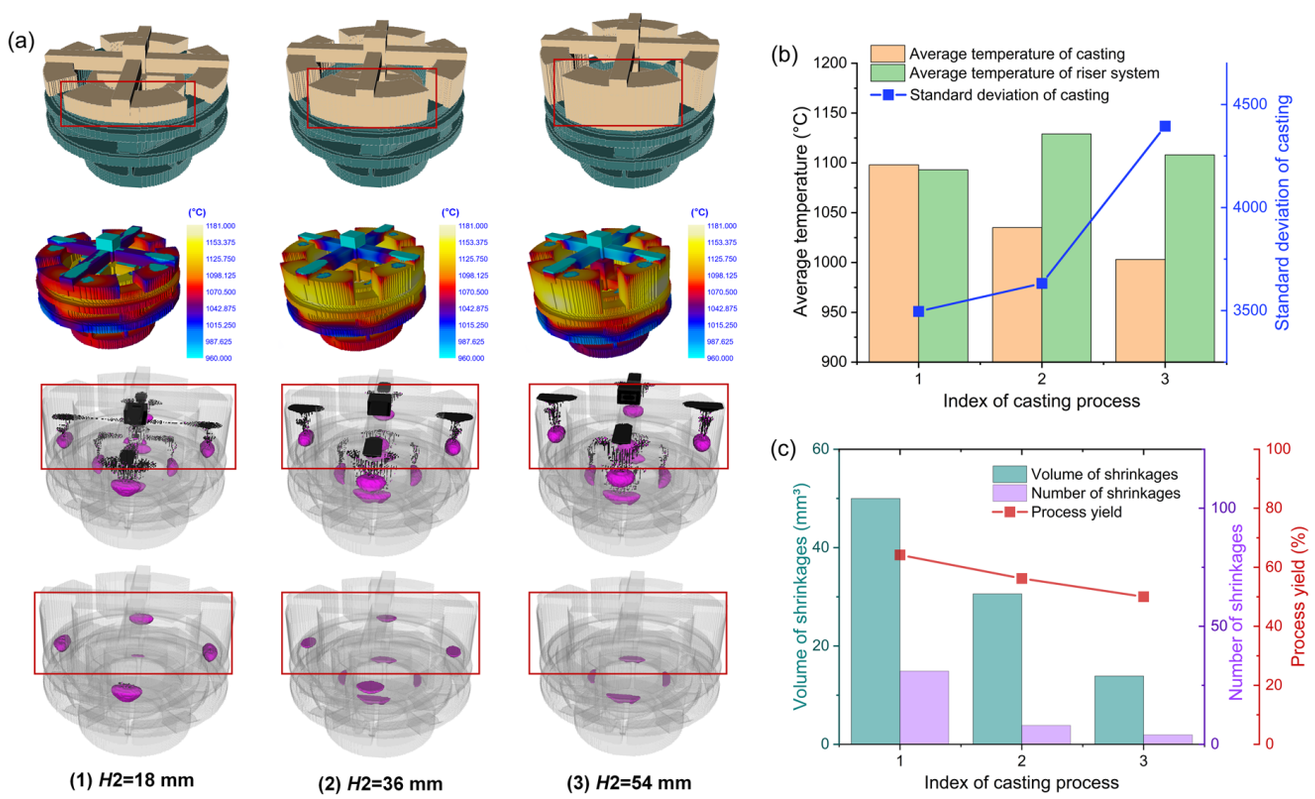

Fig. 8: Comparison of simulation results for different external riser sizes in different values of *H*2: (a) simulation results; (b) temperature field analysis; (c) shrinkage cavity analysis

fill with different outer riser sizes. Figure 8(a) illustrates the temperature field and the distribution of solidification shrinkage cavities in castings under three different outer riser sizes. The temperature field during solidification reveals that, as the outer riser size increases, the temperature at the riser remains significantly higher than that of the casting. This facilitates the riser's final solidification and promotes the discharge of shrinkage cavities from the casting. This trend is also evident in the shrinkage cavity distribution results. As the riser size increases, shrinkage cavities shift upwards, therefore, the occurrence of shrinkage cavity defects in the castings progressively decreases. Figure 8(b) provides analytical and

quantitative results for the temperature field across the three scenarios. The data indicate that, during the final stage of solidification, a larger riser size leads to a lower average casting temperature and a higher average riser temperature. This suggests that a larger riser size enhances the riser's role in final solidification, promoting the discharge of shrinkage cavities. Figure 8(c) depicts the size and volume of porosity during solidification, along with the process yield. The findings demonstrate that increasing the outer riser size significantly reduces the number and volume of shrinkage cavities. However, this also results in a marked decrease in the process yield, with the reduction being relatively substantial.

Figure 9(a) presents a comparison of simulation results for different inner riser sizes. Among the three process schemes, Process (2) increases only the cross-sectional width of the inner riser compared to Process (1). In contrast, Process (3) increases only the riser height compared to Process (2). This design allows for evaluating both the effects of inner riser size on casting formation and the relative influence of the two variables: inner riser cross-sectional width and height. An analysis of the temperature fields for the three processes shows a clear difference between Process (1) and Processes (2) and (3). In Process (1), the temperature in the riser is significantly lower than in the casting, preventing sequential solidification. This issue is also evident in the shrinkage prediction results displayed in Fig. 9(c).

Figures 9(b) and (c) further illustrate the analytical results for the temperature field and the shrinkage pore distribution under the three processes. The results indicate that variations in the cross-sectional width of the inner riser (*D*4) result in greater changes to the temperature field compared to variations in riser height (*H*1). Therefore, the width of the inner riser has a more significant influence on the temperature field than its height. It is evident that increasing the inner riser width significantly reduces both shrinkage and porosity, underscoring its decisive role in mitigating these defects. However, increasing the riser height (*H*1) from 14 mm to 28 mm does not significantly reduce casting shrinkage and instead decreases the process yield. This indicates that increasing the inner riser width is a more crucial factor for minimizing shrinkage in the casting.

3.4 Design results and experimental verification

After considering factors such as defect formation and process yield, the optimization results of various structural parameters are obtained. The parameters which have a relatively large impact on casting defects are *H*1, *H*2, *D*2, and *D*5. In contrast, *H*3, *D*1, *D*3, and *D*4 have less influence on casting defects. In terms of riser size, the overall height of the inner and outer risers (*H*1 and *H*2) is the key parameter, while *H*3 only determines the proportion of the lower and upper part of the outer riser, which indicates that the filling path of the metal liquid in the riser is mainly related to the overall height of the riser. In terms of the dimensions of the gating system, the key parameters are the cross-sectional area (*D*2) of the cross runner and the gate neck (*D*5), while the influence of other parameters is relatively small. The main reason why *D*2 affects defect formation is that it changes the overall pouring time, which affects the temperature field at the end of pouring. The main reason why *D*5 affects the defect formation is that it changes the flow path and thus affects the solidification process. Therefore, the above key parameters (*H*1, *H*2, *D*2, *D*5) can be precisely recommended to achieve the best

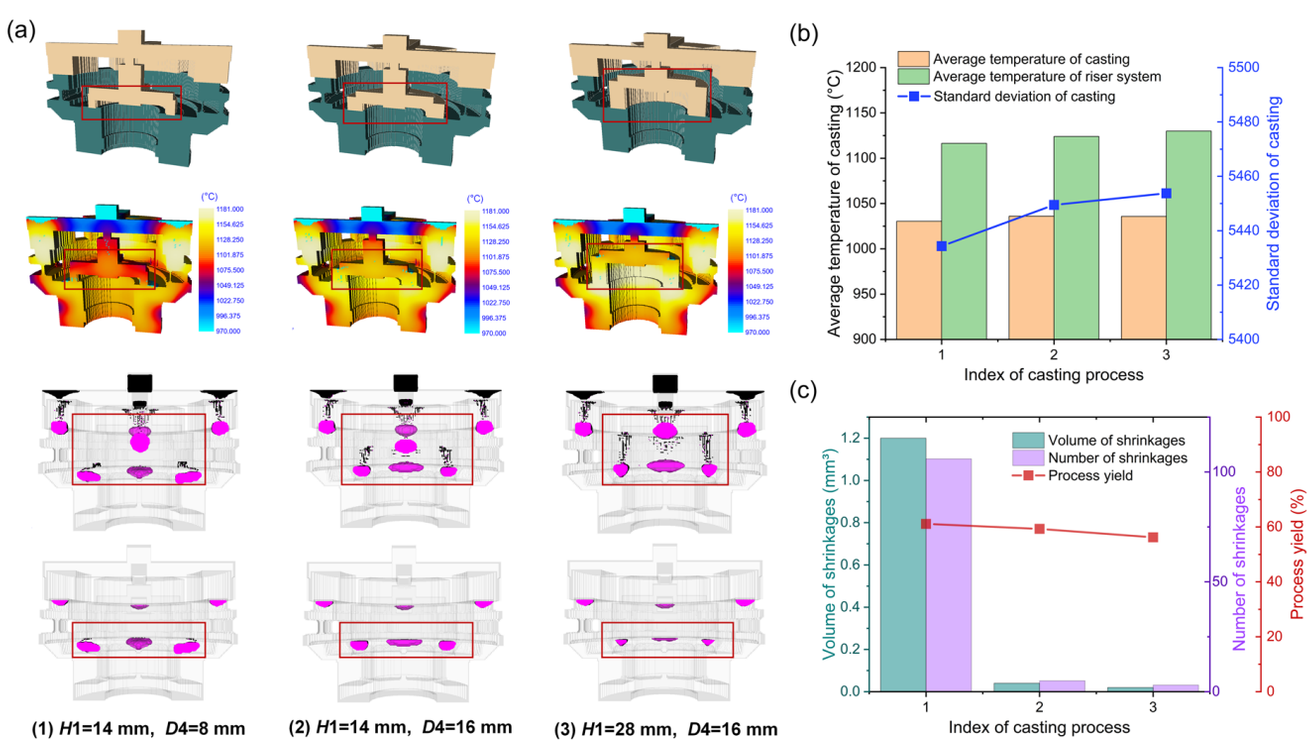

Fig. 9: Comparison of simulation results for different internal riser sizes in different values of *H*1 and *D*4: (a) simulation results; (b) temperature field analysis; (c) shrinkage cavity analysis

optimization results. For the other parameters, because of their little influence on the defect formation, only a recommended range can be given, and the specific determination depends on the specific technological process and the convenience of manufacturing. The design results of the structural parameters are summarized in Table 5, with the 3D design results shown in Fig. 10. The simulation results indicate that shrinkage defects in the casting are effectively controlled, with almost no shrinkage cavities forming within the casting.

To verify the automatic process design results and simulation results above, the investment casting experiment was carried out. In this experiment, the optimal design results of the gating and riser system obtained by the model were selected for the casting experiment. The superalloy used is K4169 and the shell slurry used is corundum and bauxite. The pouring temperature is 1,500±10 °C, the pouring time is 5 s, and the preheating temperature of the shell is 800 °C. In terms of quality inspection, X-ray testing is adopted to detect internal shrinkage cavity and porosity in castings.

Figure 11 illustrates the experimental results of the final design scheme, which involves designing the gating and riser system, fabricating the wax pattern, producing the shell mold, and finally manufacturing the casting. The surface topography of the casting was analyzed, and the result is shown in Fig. 11(c), the casting surface is smooth with no visible defects. Compared with the original pouring system and riser system, the process yield is increased from 42% to 57%.

Figure 12 shows the distribution of shrinkage cavities in the internal riser. In Fig. 12, the red circle marks the casting area, while the red outline represents the riser area. It is evident that most defects have been eliminated from the casting. The simulation results shown in Fig. 11(b) indicate numerous

Table 5: Design results of structural parameters

Structural parameter	*H*1 (mm)	*H*2 (mm)	*H*3 (mm)	*D*1 (mm)	*D*2 (mm)	*D*3 (mm)	*D*4 (mm)	*D*5 (mm)	Riser_Num	Angle_Rate
Recommended value	28	54	16–20	30–34	16	50–60	12–18	18	3–6	0.2–0.4
Experimental value	28	54	18	32	16	56	16	18	4	0.3

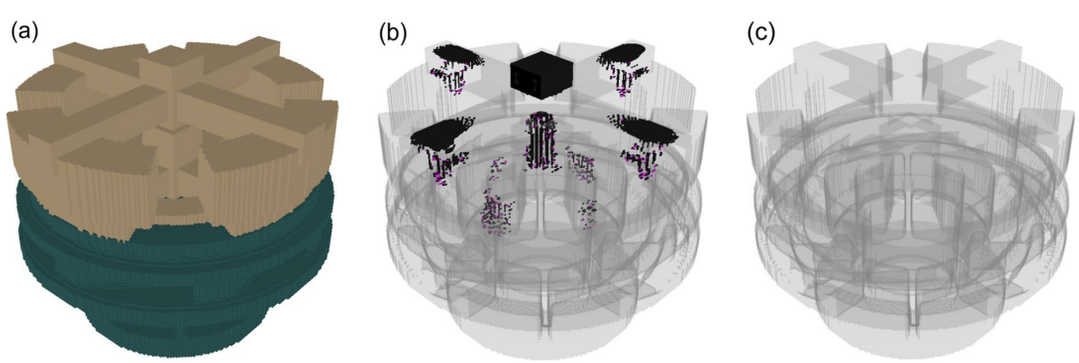

Fig. 10: Final design results and its shrinkage prediction results: (a) gating and riser system design results; (b) shrinkage distribution results in the gating system and risers; (c) shrinkage distribution results in castings

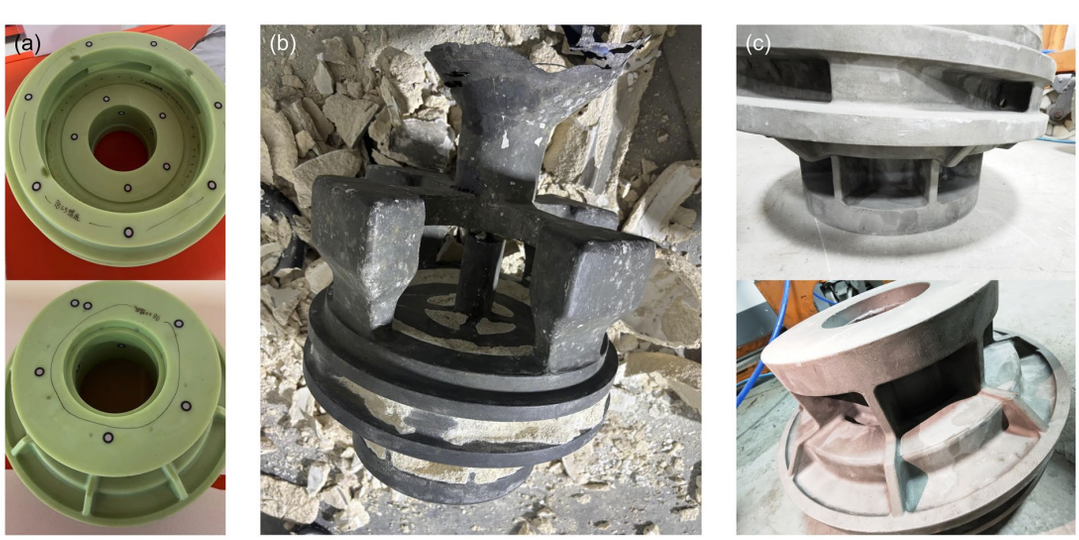

Fig. 11: Experimental verification of final design: (a) wax pattern fabrication; (b) gating and riser system; (c) final casting product

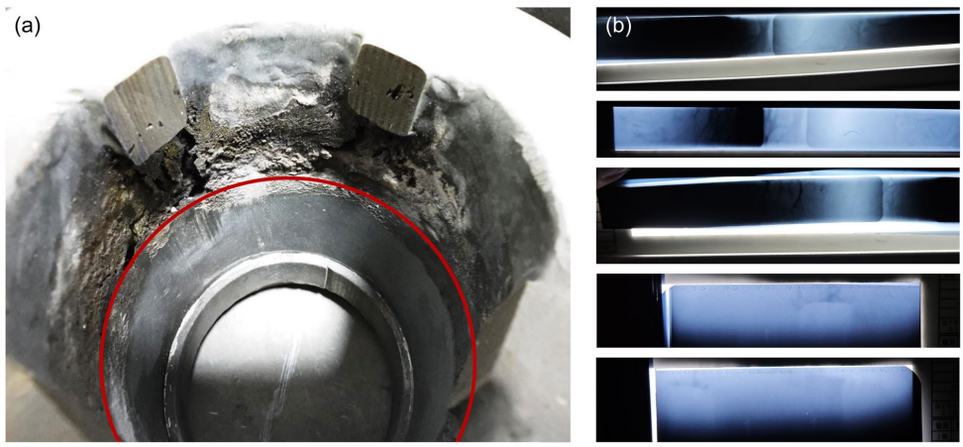

Fig. 12: Shrinkage cavity distribution on casting surface (a) and inside the casting (b) as detected by X-ray

defects in the internal riser, no such defects are present in the casting, confirming that the experimental results align with the simulation findings. Figure 12(b) presents X-ray inspection results of the internal defects, showing no significant shrinkage issues inside the casting. This confirms that the designed structural parameters effectively eliminate shrinkage defects. The designed process not only increases the process yield by 15%, but also ensures the quality of the castings. The results validate the reliability of the parametric 3D modeling-simulation model.

4 Conclusions

In this work, a novel parametric 3D modeling-simulation integrated system is established. By changing ten typical structural parameters, hundreds of casting processes with different gating and feeding systems can be generated and simulated in batches. Through comparative analysis, recommended structural parameters are given, and experiments are carried out based on the recommended processes. The results show that the recommended processes eliminate all casting defects and meet the quality requirements. The following conclusions can be drawn based on this study:

(1) In the analysis of the influence of the gating system on the formation and defects of castings, when the side length of the gate neck is 18 mm, the flow rates of the two flowing branches separated by the gate neck are nearly the same, which is more likely to cause turbulence and entrained gas defects, and is not good for the quality of the castings. When the side length of the gate neck is larger (24 mm), the temperature distribution within the casting becomes more uniform, which can prevent the formation of shrinkage cavities. The increase in the cross-sectional size of the gate will lead to an increase in the flow pressure and impact force. However, the rapid filling process is conducive to maintaining the uniformity of the temperature field, the number of shrinkage cavities in the final castings will be reduced.

(2) When analyzing the influence of the riser system on the defects of the castings, increasing the size of the external riser eliminates most of the internal shrinkage cavities in the castings. On the contrary, increasing the size of the internal riser does not significantly eliminate the internal shrinkage cavities in the castings. The reason is that the cooling and heat dissipation law of the external riser is more in line with the sequential solidification pattern, while the heat diffusion of the internal riser is relatively slow. Therefore, the function of the riser cannot be fully exerted.

(3) Based on the results of the comparative simulation analysis, the recommended process parameters are given, and casting experiments and X-ray inspections of casting defects are carried out. The designed process not only increases the process yield by 15%, but also ensures the quality of the castings. The results validate the reliability of the parametric 3D modeling-simulation model.

Acknowledgment

This work was financially supported by the National Key Research and Development Program of China (2022YFB3706802).

Conflict of interest

The authors declare that they have no known competing financial interests or personal relationships that could have appeared to influence the work reported in this paper.

References

[1] Ren J, Chen X, Li Y, et al. Properties of fiber reinforced plaster molds for investment casting. China Foundry, 2020, 17(5): 332–340.
[2] Yu P, Ji X, Sun T, et al. Data-physics fusion-driven defect predictions for titanium alloy casing using neural network. Materials, 2024, 17(10): 2226.
[3] Uwanyuze R S, Kanyo J E, Myrick S F, et al. A review on alpha case formation and modeling of mass transfer during investment casting of titanium alloys. Journal of Alloys and Compounds, 2021, 865: 158558.
[4] Hao X, Liu G, Wang Y, et al. Optimization of investment casting process for K477 superalloy aero-engine turbine nozzle by simulation and experiment. China Foundry, 2022, 19(4): 351–358.

[5] Ren S, Bu K, Mou S, et al. Control of dimensional accuracy of hollow turbine blades during investment casting. Journal of Manufacturing Processes, 2023, 99: 548–562.
[6] Kim Y, Paek N, Ri B, et al. Improvement of quality and yield for investment casting of centrifugal pump impeller by tilting mold and optimizing runner/riser system. The International Journal of Advanced Manufacturing Technology, 2024, 130(5): 2369–2379.
[7] Dejene N D, Lemu H G, Gutema E M. Critical review of comparative study of selective laser melting and investment casting for thin-walled parts. Materials, 2023, 16(23): 7346.
[8] Tao P, Shao H, Ji Z, et al. Numerical simulation for the investment casting process of a large-size titanium alloy thin-wall casing. Progress in Natural Science: Materials International, 2018, 28(4): 520–528.
[9] Xiao Z Y, Lv Z Z, Zhou X Y, et al. Numerical simulation and optimization of investment casting for complex thin-walled castings. International Journal of Metalcasting, 2024, 18(1): 159–179.
[10] Ma D. Novel casting processes for single-crystal turbine blades of superalloys. Frontiers of Mechanical Engineering, 2018, 13(1): 3–16.
[11] Dong R, Wang W, Cui K, et al. An investigation of ceramic shell thickness uniformity and its impact on precision in turbine blade investment casting. Journal of Manufacturing Processes, 2024, 131: 507–522.
[12] Gao H, Guan K, Cui R, et al. Effect of lanthanum on microstructure of a nickel-based single crystal superalloy. China Foundry, 2025, 22(1): 55–64.
[13] Fang Y, Li Y, Yang Q, et al. Oxidation behavior of 4774DD1 Ni-based single-crystal superalloy at 980 °C in air. China Foundry, 2024, 21(2): 116–124.
[14] Sui D, Shan Y, Wang D, et al. Elastic-viscoplastic constitutive equations of K439B superalloy and thermal stress simulation during casting process. China Foundry, 2023, 20(5): 403–413.
[15] Liu W, Wu Y, Gao L, et al. Pronounced impact of size and shape effects on creep rupture life of a K439B superalloy combustion chamber casting simulator. China Foundry, 2025, 22(1): 55–64.
[16] Hu Y, Ma J, Xu Q. Numerical simulation on directional solidification and heat treatment processes of turbine blades. China Foundry, 2024, 21(5): 476–490.
[17] Wei Y, Yu B, Yang Q, et al. Numerical simulation and experimental validation on fabrication of nickel-based superalloy Kagome lattice sandwich structures. China Foundry, 2020, 17(1): 21–28.
[18] Li Z, Xiong J, Xu Q, et al. Deformation and recrystallization of single crystal nickel-based superalloys during investment casting. Journal of Materials Processing Technology, 2015, 217: 1–12.
[19] Lee K, Blackburn S, Welch S T. Adhesion tension force between mould and pattern wax in investment castings. Journal of Materials Processing Technology, 2015, 225: 369–374.
[20] Konrad C H, Brunner M, Kyrgyzbaev K, et al. Determination of heat transfer coefficient and ceramic mold material parameters for alloy IN738LC investment castings. Journal of Materials Processing Technology, 2011, 211(2): 181–186.
[21] Dong R, Wang W, Cui K, et al. Core shifting prediction in filling process of hollow turbine blade investment casting. Journal of Manufacturing Processes, 2023, 86: 253–265.
[22] Kao Y C, Ho M, Tseng H W, et al. Computer-aided engineering (CAE) simulation for the robust gating system design: Improved process for investment casting defects of 316L stainless steel valve housing. International Journal of Metalcasting, 2022, 16: 2014–2032.
[23] Afazov S M, Becker A A, Hyde T H. FE prediction of residual stresses of investment casting in a Bottom Core Vane under equiaxed cooling. Journal of Manufacturing Processes, 2011, 13(1): 30–40.
[24] Li Z, Xiong J, Xu Q, et al. Deformation and recrystallization of single crystal nickel-based superalloys during investment casting. Journal of Materials Processing Technology, 2015, 217: 1–12.
[25] Wang T, Shen X, Zhou J, et al. Optimal gating system design of steel casting by fruit fly optimization algorithm based on casting simulation technology. International Journal of Metalcasting, 2019, 13: 561–570.
[26] Dučić N, Ćojbašić Ž, Manasijević S, et al. Optimization of the gating system for sand casting using genetic algorithm. International Journal of Metalcasting, 2017, 11: 255–265.
[27] Jezierski J, Dojka R, Janerka K. Optimizing the gating system for steel castings. Metals, 2018, 8(4): 266.
[28] Wang T, Yin Y, Zhou J, et al. Optimal riser design method based on geometric reasoning method and fruit fly optimization algorithm in CAD. The International Journal of Advanced Manufacturing Technology, 2018, 96(1–4): 53–65.
[29] He B, Lei Y, Jiang M, et al. Optimal design of the gating and riser system for complex casting using an evolutionary algorithm. Materials, 2022, 15(21): 7490.
[30] Malik I, Sani A A, Medi A. Study on using casting simulation software for design and analysis of riser shapes in a solidifying casting component. Journal of Physics: Conference Series, 2020, 1500: 012036.
[31] Wang D, Sun J, Dong A, et al. An optimization method of gating system for impeller by RSM and simulation in investment casting. The International Journal of Advanced Manufacturing Technology, 2018, 98: 3105–3114.
[32] Wang Y F, Shan Z D, Yang H Q, et al. Optimization of casting process of headstock based on numerical simulation. Journal of Physics: Conference Series, 2021, 1802: 022096.
[33] Vanikar N P, Ohol S S, Goldar S. Methodology for optimization of pouring variables using bottom pour for low masses of SS304 (<300 kg) in investment casting process (case study). International Journal of Cast Metals Research, 2018, 31(4): 249–259.
[34] Yang J, Li H. Accuracy of CAD-CAM milling versus conventional lost-wax casting for single metal copings: A systematic review and meta-analysis. The Journal of Prosthetic Dentistry, 2022, 132(1): 51–58.
[35] Guan B, Wang D, Ma H, et al. Key technology and application of digital twin modeling for deformation control of investment casting. Acta Metallurgica Sinica, 2023, 60(4): 548–558. (In Chinese)